Method for sampling compact configurations for semistiff polymers

Alexey Siretskiy[*] and Christer Elvingson[†]
Department of Physical and Analytical Chemistry, Uppsala University, SE-751 23 Uppsala, Sweden

Pavel Vorontsov-Velyaminov[‡]
Faculty of Physics, St. Petersburg State University, St. Petersburg 198504, Russia

Malek O. Khan[§]
Department of Physical and Analytical Chemistry, Uppsala University, SE-751 23 Uppsala, Sweden and
FOI, Swedish Defense Research Agency, SE-164 90 Stockholm, Sweden

(Received 7 March 2011; revised manuscript received 6 April 2011; published 7 July 2011)

The sampling of compact configurations is crucial when investigating structural properties of semistiff polymers, like proteins and DNA, using Monte Carlo methods. A sampling scheme for a continuous model based on configuration biasing is introduced, tested, and compared with conventional methods. The proposed configuration biased Monte Carlo method, used together with the Wang-Landau sampling scheme, enables us to obtain any thermodynamic property within the statistical ensemble in use. Using the proposed method, it is possible to collect statistical data of interest for a wide range of compactions (from stretched up to several toroid loops) in a single computer experiment. A second-order-like stretched-toroid phase transition is observed for a semistiff polymer, and the critical temperature is estimated.

DOI: 10.1103/PhysRevE.84.016702 PACS number(s): 05.10.Ln, 05.20.Gg, 82.20.Wt, 64.60.De

I. INTRODUCTION

The use of computer simulations to investigate the structure of macromolecules is a rather well developed area for many types of polymers [1–7]. In cases when the system under investigation undergoes an essential change in geometry (for example, a phase transition), conventional Metropolis Monte Carlo (MC) is not an efficient simulation method [1]. One way to improve the efficiency is to include a configurational bias. It is a useful tool when modeling gas-liquid phase transitions for simple ionic liquids in the framework of the restricted primitive model [8] as well as when studying configuration properties of semistiff polymers [1].

Configuration biased Monte Carlo (CBMC) methods are suitable when performing polymer simulations in order to sample configurations which are confined in a general way. Confinement can be straightforward: due to the physical size of the boundaries of the system [2]. As an example, one can consider tightly packed viral DNA in the capsid whose dimensions are comparable with the persistence length of DNA [3]. Another type of confinement is due to a high concentration of surrounding molecules. In this case, most of the attempts to change the geometry of the chain will be doomed due to steric factors (overlapping). The polymer also can become more compact due to the presence of compaction agents [4].

There are several types of chain moves which are widely used in computer simulations of polymer systems. For continuous models, pivot moves [9], crankshaft, and single bead (monomer) displacements are traditionally used to achieve efficient sampling [5]. A common problem for all these moves is that they fail for dense systems [10] and can not be used to produce compact configurations, especially in the case of semistiff polymers [1]. This is the main reason why the problem of thermodynamic stability for compact conformations of semistiff polymers still is not solved computationally.

Nevertheless, some studies of conformation stability for compact polymers have been carried out using both molecular dynamics (MD) and MC methods. In MD, the initial configuration is prepared in the conformation under investigation (e.g., toroid, globule, or cigar), and during the simulation, the stability of the given structure is observed [11]. In the MC approach, it is possible to prepare the system in a compact state and then try to move parts of it in small displacements [12]. If the system is in a stable state (minimum in free energy), it will fluctuate around this state or else degrade in the case of a badly guessed initial configuration. Another way to investigate stability is to release the polymer and let it find the stable state itself while modifying its geometry throughout the experiment [1,5]. In this case, it is crucial how the geometry changes are performed, since it has been shown that it is hardly possible to sample structures more compact than two coils of toroidal-like or cigarlike conformations with only clothed pivot and crankshaft moves [1].

An alternative to the pivot moves is a bead-by-bead regrowth of an entire chain. The orientation of each monomer is governed by the configuration bias used. This sampling technique showed high efficiency in the case of lattice models for flexible polymers [6]. In the present work, we have extended the model to include the stiffness of the chain. We also used a continuous model where the number of orientations is not determined by the structure of the underlying lattice.

It is shown that a CBMC method applied to semistiff polymers in a continuous model can shed light on the problem of sampling compact toroidal-like configurations.

[*]alexey.siretskiy@fki.uu.se
[†]christer.elvingson@fki.uu.se
[‡]voron.wgroup@gmail.com
[§]malek.khan@fki.uu.se

The paper is organized as follows: in Sec. II, the Rosenbluth ideas of configuration generation of polymer systems are briefly described and some modifications are introduced. The Wang-Landau sampling technique is coupled with the Rosenbluth sampling, and formulas for the transition probabilities are derived. In Sec. III, the model used is described and tested using well-known techniques. The details of the implementation are also discussed. In Sec. IV, the newly derived method is applied to a semistiff polymer with a torsion stiffness. The phase transition temperature is estimated. In the last section, we summarize the major features of our method as well as some points for future development of the presented method.

II. ROSENBLUTH SAMPLING APPLIED TO SEMISTIFF POLYMERS

Computer simulations of semistiff polymers, with the goal of collecting statistical properties for a wide range of chain compactions, face two main problems: how to generate the compact configurations and how to force the system to explore a wide range of compactions (from several loops to an uncoiled structure). In order to solve both these problems, we introduce two biases, one configurational in order to construct compact configurations and another forcing the system to coil and uncoil during the MC simulation. The former is referred to as a Rosenbluth-like biasing [13], and the latter is the Wang-Landau biasing scheme [14]. One should mention that for *flexible chains* the problem of compaction is less difficult, and it has been solved in continuous models [15,16] as well as for lattice models [17].

A. Rosenbluth-like sampling

An elegant technique for sampling polymer configurations was introduced by Rosenbluth and Rosenbluth in 1955 [18]. The main drawback of the initial idea was that it leads to a non-Boltzmann sampling [13,19]. It means that during a simulation with this sampling technique, the generated configurations are not Boltzmann distributed, and some corrections were needed. A more recent technique involving Rosenbluth sampling was introduced by Frenkel *et al.* [20]. This method allows the generation of Boltzmann-distributed configurations, and it can be used in an ordinary CBMC simulation.

The ideas described above are very general and can be modified if needed. It is possible to construct your own Rosenbluth-like factors in order to introduce a configuration bias to the MC sampling procedure. To produce compact configurations of a polymer chain, the temperature dependent biasing Rosenbluth factor as introduced in [20] is, however, not efficient enough for these cases, and stronger conditions for constructing a biasing factor are needed.

We introduce here a new Rosenbluth-like factor

$$W(\lambda) = \prod_{i=1}^{l-1} w_i(\lambda), \tag{1}$$

where l is the number of beads in the chain, and

$$w_i(\lambda) = \sum_{j=1}^{k} \exp\left[-\lambda u_i^r(j)\right], \tag{2}$$

where λ is a numerical factor, k is the number of trial orientations for every monomer, and $u_i^r(j)$ is a construction of type:

$$u_i^r(j) = 1 - \frac{u_i(j)}{\min_{j=1}^{k}\{u_i(j)\}}, \tag{3}$$

where $u_i(j)$ is the interaction energy between monomer i in the trial position j and the *already grown* part of the chain. The type of construction in Eq. (3) was chosen to transform nonbonded energies to the interval $[0:\infty)$. For example, $u_i^r(j) = 0.0$ for the lowest of $u_i(j)$, and ∞ for overlapping configurations.

So, among the k trial configurations, one is selected with a probability [21]

$$p_i(\lambda,u) = \frac{e^{-\lambda u_i^r(j)}}{w_i(\lambda)}. \tag{4}$$

As it can be seen from Eq. (4), the smaller (more negative) the nonbonded interaction energy between a trial position of the monomer and the *already* grown part of the chain is, the larger is the probability of selecting a given trial position. This will result in the generation of a compact structure by setting up the corresponding parameter λ *regardless* of the temperature. If $\lambda = 0.0$, it will mean that we do not favor selecting compact structures, and all trial configurations are equiprobable. If $\lambda > 0$, for example, $\lambda = 20.0 - 50.0$, $p_i(\lambda,u)$ is peaked around 0, and we will mostly select such trial configurations which result in very compact structures. A more detailed discussion about the choice of λ will be given in Subsec. IV B.

Sometimes, however, especially for long chains, *all* trial orientations will result in overlapping configurations, the so called *dead-valley problem*. In this case, Eq. (3) will not work, and we will regrow the chain from start. This does not introduce any additional biasing in the scheme, though, since we are accumulating data for nonoverlapping configurations.

B. Wang-Landau sampling technique with Rosenbluth sampling

As mentioned above, Rosenbluth-like sampling allows one to generate compact configurations. Moreover, the degree of compactness is governed by λ, which is an input parameter and can be varied. It means that one can find or select a λ, which provides sampling of configurations with various levels of compactness.

A problem is that these stable structures have a local free energy minimum, so once the system finds itself in such a state, it will spend many MC steps there. It also means that other parts of the configurational space will remain unexplored.

Fortunately, the Wang-Landau (WL) sampling technique provides a way to circumvent this drawback. The idea behind WL is that the less probable it is for a state to be visited, the higher the acceptance probability for this state becomes. Applying this to polymer configurations means that even if the system falls into a stable state, sooner or later it will be forced to leave it by the dynamically changing acceptance rate in the WL procedure [14]:

$$\pi[o \to n] = \min\left[1, \frac{\Omega(E_o)}{\Omega(E_n)}\right], \tag{5}$$

where $\Omega(E_o)$ and $\Omega(E_n)$ are the energy densities of the old and new states, respectively. The density of energy states is defined as $\Omega(E) = \int \delta(E - U(q))dq$, where dq denotes the differential of the configurational space, and $U(q)$ is the potential energy of the given configuration q. It should be noted that Eq. (5) can be applied only in the case when we select trial configurations *randomly*, which is not true in our case, and some modifications are needed.

Let us apply the idea of WL sampling to the Rosenbluth procedure for generating configurations. We follow the notation from Frenkel and Smit [13]. Detailed balance as a configuration flow can be described as

$$K(o \to n) = K(n \to o), \tag{6}$$

where $K(o \to n)$ and $K(n \to o)$ are the numbers of accepted moves (on average) from old to new and from new to old configurations, respectively. Equation (6) can be factorized according to

$$K(o \to n) = p(o)\alpha(o \to n)\pi(o \to n), \tag{7}$$

where $p(o)$ is the probability for a system to be found in the given state $\{p(o) \propto \exp[-\beta U(o)]$ for the canonical ensemble$\}$, $\alpha(o \to n)$ is the probability of selecting a new configuration (referred to as the Markov's transition matrix), and $\pi(o \to n)$ is the probability of accepting a move from an old to a new state.

In our case, we bias the configurations in two ways. First, we introduce a Rosenbluth-like bias $\alpha_R(o \to n) = e^{-\lambda(n)\Re(n)}/W[n,\lambda(n)]$, and after that a bias from the WL scheme: $\alpha_{WL}(o \to n) = Q(l,V,T)/e^{-\beta E(o)}\Omega[E(o)]$ [22]. The result is

$$\frac{e^{-\beta E(o)}}{Q(l,V,T)}\frac{e^{-\lambda(n)\Re(n)}}{W[n,\lambda(n)]}\frac{Q(l,V,T)}{e^{-\beta E(o)}\Omega[E(o)]}\pi(o \to n) = \frac{e^{-\beta E(n)}}{Q(l,V,T)}\frac{e^{-\lambda(o)\Re(o)}}{W[o,\lambda(o)]}\frac{Q(l,V,T)}{e^{-\beta E(n)}\Omega[E(n)]}\pi(n \to o), \tag{8}$$

where λ is the compactness factor, $W(\lambda)$ is defined in Eq. (1), $\Omega(E)$ is the energy density of states, and $\Re$ is the reduced nonbonded energy of the chain [23]:

$$\Re = \sum_{i=1}^{l} u_i^r. \tag{9}$$

After simplifications, Eq. (8) can be written [6,24]

$$\pi(o \to n) = \min\left[1, e^{\lambda\Delta\Re}\frac{W[n,\lambda(n)]}{W[o,\lambda(o)]}\frac{\exp(S(E_o))}{\exp(S(E_n))}\right], \tag{10}$$

where the relation $S = k_B \ln\Omega$ was used.

Provided that $\Re$ and W converge during the iterative WL procedure, S also converges to some value which is the configuration entropy of the chain up to some additive constant. Similar ideas for a lattice polymer model were introduced in [6].

Special attention should be paid to the fact that $S = S(E,V,l)$, where E, V, and l are the energy, volume of the simulation cell, and number of beads in the chain, respectively, but S is not a function of λ. It should also be mentioned that in the initial scheme [13], it was proposed to *retrace* the old configuration of the existing chain to determine its Rosenbluth factor. In our case, we have just one chain, which we fully regrow to get a new configuration. In this case, we calculate W for the initial conformation, $W(o) = W$, *fully* regrow the chain, and calculate $W(n)$ for this. One MC step in our case is a bead-by-bead construction of the whole chain.

III. THE MODEL

To test the method described above, a freely rotating chain was chosen because of its simplicity and ability to form compact structures. Many analytical results also can be derived for this model. The limiting case of the freely rotating chain is a wormlike polymer, which has proven to be a very suitable model for stiff polymers, such as DNA [25].

Other models, with an implied bending stiffness like the freely jointed chain with a bending and torsion potential are more complicated and require more input parameters. In the freely rotating chain model, it is also possible to introduce a torsional stiffness [see Eq. (17) and Fig. 1].

The input parameters for the freely rotating chain without torsional stiffness are the number of beads, l, the bond length b, and the angle between consecutive bonds, θ. A number of structural features of the chain can also be calculated analytically [26]. The mean square end-to-end distance is

$$\left\langle R_{ee}^2(N,b,\alpha)\right\rangle = Nb^2\left(\frac{1+\alpha}{1-\alpha} + \frac{2\alpha}{N(\alpha-1)^2}(\alpha^N - 1)\right), \tag{11}$$

and the mean square radius of gyration is

$$\langle R_g^2(N,b,\alpha)\rangle = Nb^2\left[\frac{1}{6}\left(\frac{1+\alpha}{1-\alpha}\right)\frac{(N+2)}{(N+1)} + \frac{2\alpha^3(\alpha^N-1)}{N(N+1)^2(\alpha-1)^4} - \frac{N\alpha^2}{(N+1)^2(\alpha-1)^3} - \frac{\alpha}{(N+1)(\alpha-1)^2}\right], \tag{12}$$

where $\alpha = \cos\theta$ and $N = l - 1$ is the number of bonds.

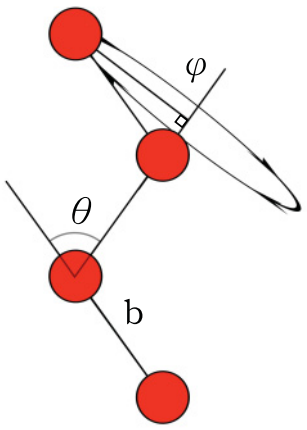

FIG. 1. (Color online) Segment of the chain. The angle θ and the bond length b are parameters of the chain. The torsional angle φ can provide a torsion stiffness according to Eq. (17).

TABLE I. $\sqrt{\langle R_g(N)^2\rangle}$ dependence for the freely rotating model. Data obtained for $b = 3$ and $\alpha = 0.875$ ($\theta \approx 29^\circ$). The forth column shows the importance of using the exact relation [Eq. (12)] instead of the approximate equation.

	$\sqrt{\langle R_g(N)^2\rangle}$		
N	Exact, Eq. (12)	Averaged, Eq. (14)	Eq. (12) with $N \gg 1$
19	13.84	13.82	20.68
29	18.99	18.92	25.54
39	23.44	23.29	29.62
49	27.37	27.19	33.20
59	30.92	30.93	36.43
69	34.16	34.12	39.40

During the simulation, $\langle R_g^2\rangle^{1/2}(i)$ for the ith energetic interval was accumulated using

$$\left\langle R_g^2(i)\right\rangle = \frac{1}{N_{MC}} \sum_{j=1}^{N_{MC}} R_g^2(j)(i), \tag{13}$$

where N_{MC} is the number of MC visits to the ith energetic interval. After convergence of the simulation, the result of

$$\sqrt{\langle R_g^2\rangle} = \frac{\sum_i \sqrt{\langle R_g^2(i)\rangle} e^{S(E_i)}}{\sum_i e^{S(E_i)}} \tag{14}$$

was compared to the exact result [Eq. (12)]. Good agreement between our results and the analytical value for a phantom chain (bead size equals to 0) can be seen from the Table I.

To investigate compact structures, Lennard-Jones (LJ) interactions were used for nonbonded interactions between the beads of the chain:

$$U(r) = 4\epsilon[(a/r)^{12} - (a/r)^6], \tag{15}$$

where ϵ is the potential well depth and a is the bead diameter.

Reduced dimensionless parameters were used with the size of the bead, a, as the unit of length and ϵ as the unit of energy. In "reduced units," the LJ interactions become

$$\begin{aligned} U(r) &= 4\epsilon[(a/r)^{12} - (a/r)^6] \\ &= 4\epsilon[(1/r^*)^{12} - (1/r^*)^6] = \epsilon U^*(r^*), \end{aligned} \tag{16}$$

where $U^*(r^*) = 4[(1/r^*)^{12} - (1/r^*)^6]$ and $r^* = r/a$.

The torsion energy between the planes formed by the bond vectors $(\mathbf{r}_i, \mathbf{r}_{i+1})$ and $(\mathbf{r}_{i+1}, \mathbf{r}_{i+2})$ can be written (see Fig. 2)

$$U^*_{\text{tor}} = G\{[(\mathbf{r}_{i+1} \times \mathbf{r}_i) \cdot (\mathbf{r}_{i+2} \times \mathbf{r}_{i+1})]/C + 1.0\}, \tag{17}$$

where $[\cdot]$ stands for the dot product and $(\times)$ for the vector product. The constant $C = [\mathbf{r}_{i+1} \times \mathbf{r}_i]^2 = [\mathbf{r}_{i+2} \times \mathbf{r}_{i+1}]^2$, and G is a dimensionless quantity defining the amplitude of the torsion energy. The latter energy is shifted, so that the lowest torsion energy is 0 when the chain has the largest end-to-end distance $R_{\text{ee}} = Nb\cos(\theta/2)$. The full configuration energy in "reduced units" thus becomes:

$$U^*_{\text{tot}} = U^*(r^*) + U^*_{\text{tor}}. \tag{18}$$

In the rest of this text, the asterisk sign will be omitted.

IV. RESULTS

A. Comparison with pure Wang-Landau

To show that S is not a function of λ, a compactness parameter $\lambda > 0.0$ was chosen [27]. The result for the configuration entropy $S(E)$ is shown in Fig. 3(a). To show that for short chains, both methods, Eqs. (5) and (10), sample the same (on average) configurations, $R_g(E)$ was accumulated during the simulations and is shown in Fig. 3(b). The small difference in results between the two methods can be estimated by looking at the insets in the figures. For this test case, the most stretched and the most compact configurations are shown in Fig. 4.

B. The choice of λ

The choice of the compaction parameter λ is important as it can be seen in Eq. (4), that the larger λ is, the faster the probability will decay. It was mentioned above that $\lambda = 0.0$ corresponds to the case in which we choose the trial orientation randomly. If a large $\lambda > 0.0$ is chosen, one would sample *mostly* compact configurations. It is also true that the configuration entropy $S(l, V, E)$ does not depend on λ, and, in principle, it is possible to *change* the compaction parameter λ during the simulation. Fortunately, the choice of this convergence parameter λ can be done in a smart way. It is possible to find a value of λ, such that the probabilities for *all* the k trial orientations are about the same magnitude. Since the probabilities for all k trial orientations do not differ by

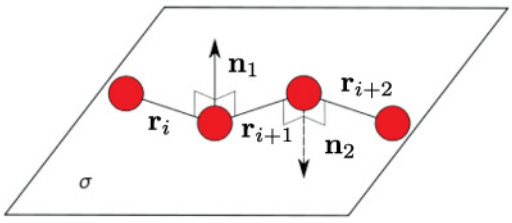

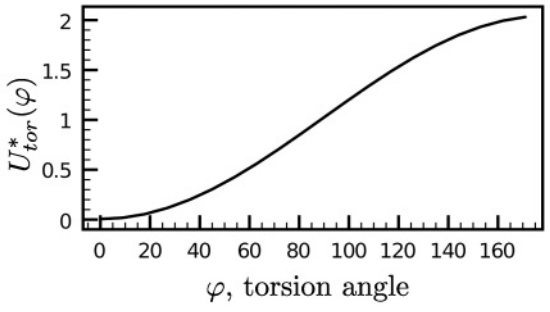

FIG. 2. (Color online) Illustration of Eq. (17). Left: the direction of the vector product of $\mathbf{r}_{i+1}$th and $\mathbf{r}_i$ bond vectors is denoted as $\mathbf{n}_1$. The direction of the corresponding vector product for $\mathbf{r}_{i+2}$ and $\mathbf{r}_{i+1}$ is denoted as $\mathbf{n}_2$. The normals $\mathbf{n}_1$ and $\mathbf{n}_2$ are perpendicular to the plane σ, which contains the centers of the beads. One can see that for such a configuration, Eq. (17) gives $U^*_{\text{tor}} = 0.0$. Right: the graph corresponding to Eq. (17) is shown.

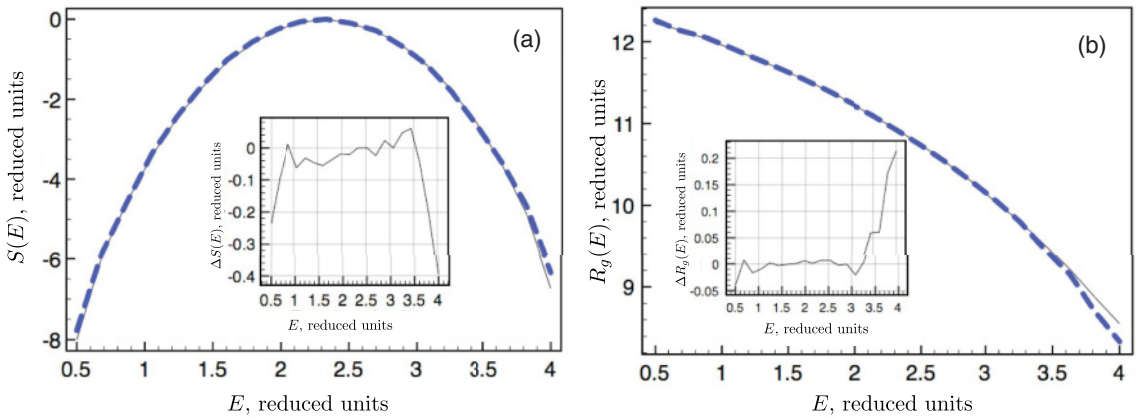

FIG. 3. (Color online) (a) Configuration entropy as a function of energy, $S(E)$, and (b) radius of gyration as a function of energy, $R_g(E)$, obtained by Eq. (5) (thin line) and by Eq. (10) (thick dashed line). In the inset of (a), the difference $\Delta S = S[\text{Eq. (10)}] - S[\text{Eq. (5)}]$ in the common energy interval is shown. The parameters are $l = 15$, $\lambda = 15.0$, $G = 0.2$, $\alpha = 0.875$ ($\theta \approx 29^\circ$), $b = 3.0$, and $k = 20$.

many orders in magnitude, it is possible to get *both* compact and prolonged configurations with a carefully chosen value of λ. The usual drawback of this kind of biasing is the necessity to be able to estimate a suitable value before doing the experiment. As a possible way for systematically selecting λ, we can use the following procedure. First, estimating the range $[R_g^{\min} : R_g^{\max}]$ and calculating the approximate energies $[E_{\min} : E_{\max}]$ for these R_g borders. The range of energies will provide the borders for $S(E)$, and λ can then be adjusted to visit $[R_g^{\min} : R_g^{\max}]$ in an efficient way.

C. Proper sampling of the configuration space

The sampling of the configuration space can be projected to the range of R_g values visited throughout the simulation. The R_g range for the self-avoiding configurations was divided into 100 intervals. The number of visits to the different R_g intervals for both schemes, Eq. (5) with one MC step as a tail rotation and Eq. (10) with one MC step being a full chain regrowth, are shown in Figs. 5(a) and 5(b), respectively. One can notice that even after $100 \cdot 5000 = 500\,000$ tail rotations following Eq. (5), the most compact states are still unvisited, while using Eq. (10), it is enough to perform $100 \cdot 100 = 10\,000$ chain regrowths to sample all R_g intervals. The structures approximately corresponding to the first 5 and last 5 of the R_g intervals are shown in Fig. 6.

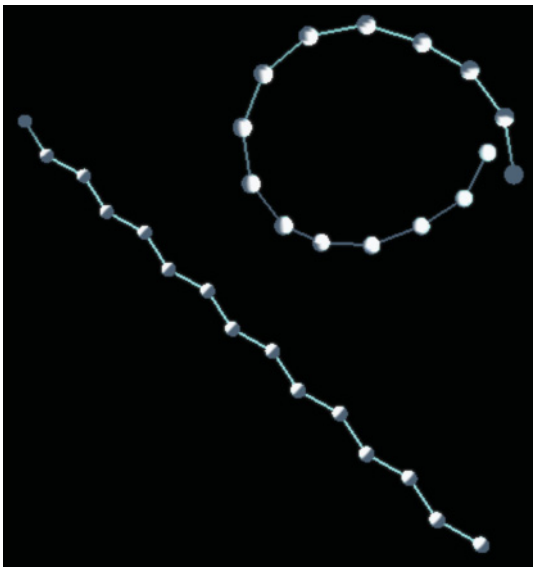

FIG. 4. (Color online) Most compact and the most prolonged configurations for a short chain: $l = 15$, $\theta \approx 29^\circ$, and $b = 3.0$.

D. Computational aspects

With an inappropriate choice of parameters, the Markov chain converges to its steady state very slowly, which means that the simulation will not give correct results in finite time. For example, too small particle displacements in the MC simulation of a molecular liquid will result in very slow mixing and equilibration, while too big steps will result in a large number of overlaps significantly reducing the efficiency.

In this work, the important simulation parameters are the number of intervals, N_b, in the desired energy range $[E_1 : E_2]$, the number of trial orientations for each bead, k, and the compaction factor λ.

We found that for a chain length $l \in [15 : 80]$ and torsion stiffness $G \in [0.00 : 0.40]$ the energy range of interest is $E \in [-30.0 : 30.0]$ in "reduced units." We also observed that it is reasonable to choose the number of energy intervals of order $N_b \in [20 : 100]$. A larger N_b influences the speed of convergence significantly. The number of trial orientations is $k \in [5 : 50]$. Generally, the longer the chain, the larger the number of trial orientations should be used for good sampling.

The Wang-Landau algorithm demands additional parameters to be specified. Two types of counters are used: one vector for the visits of the energy intervals E_i and another for the accumulation of entropy $S(E_i)$. During a simulation, the first counter is updated for every visit to a specific energy interval, while for the entropy counter, we use $S(E_i) = S(E_i) + \Delta S$, where ΔS is initially set to $\Delta S = 1.0$. After the histogram representing the number of visits becomes flat, the first counter is reset to 0, and ΔS is reduced to $\Delta S = \Delta S/2$. The simulation is terminated when ΔS becomes less than some predefined small number.

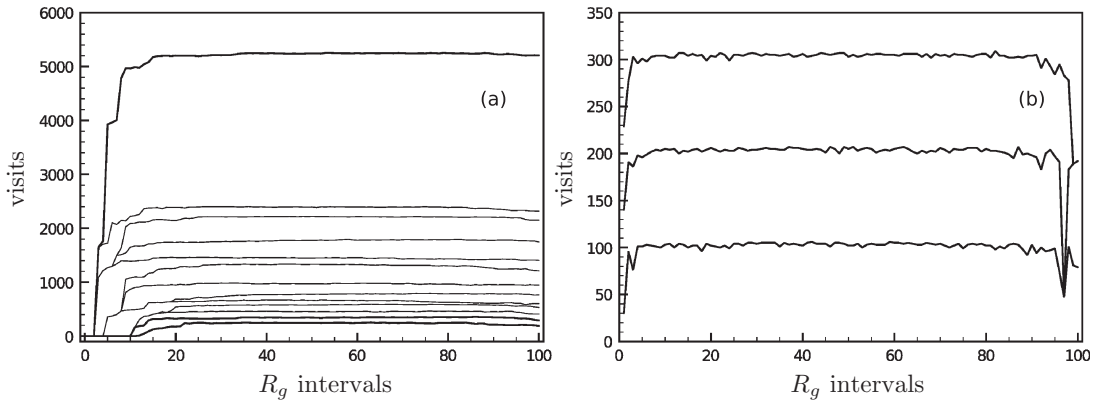

FIG. 5. (a) Visits of the R_g intervals during an experiment with the scheme using Eq. (5), and (b) the scheme using Eq. (10). The chain length is $l = 60$ with $\theta \approx 29^\circ$, $b = 1.0$, $k = 10$, and $\lambda = 15.0$.

There is no unambiguous connection between the configurational energy and the configuration. For example, different configurations can have energies falling into the same energy interval. A similar situation is with the configurational bias: factors like $W(\lambda)$ and $\Re$ in Eq. (10) are slightly different for the same energy interval and do *not* converge for the ith energy interval, while the *energy density of states* $\Omega(E_i)$ *converges* for a given interval, according to its physical sense. This divergence *does not* allow the sampling scheme to converge, forcing us to use the fact that a quantity like $\langle W(\lambda)/e^{-\lambda\Re}\rangle$ has an *average* which *converges for every energy interval*, so it is possible to use the *average*

$$\Psi(\lambda) = \langle W(\lambda)/e^{-\lambda\Re}\rangle \tag{19}$$

FIG. 6. Example of a compact and a prolonged structure, generated using Eq. (10). The system is $l = 60$, $\theta \approx 29^\circ$, $k = 10$, and $\lambda = 15.0$.

in Eq. (10) to make the resulting curve $S(E)$ *smoother*. The assumption we made, however, is shown to work by the results shown in Fig. 7. In this case, Eq. (10) can be written

$$\pi(o \to n) = \min\left[1, \left\langle \frac{W[n,\lambda(n)]}{e^{-\lambda(n)\Re(n)}}\right\rangle \left\langle \frac{e^{-\lambda(o)\Re(o)}}{W[o,\lambda(o)]}\right\rangle \frac{\Omega(E_o)}{\Omega(E_n)}\right]. \tag{20}$$

All the simulations were performed according to formula [Eq. (20)]. After these preparations, the curves $S(E)$ were used for calculating thermodynamic averages.

We also made sure to control the correctness of the approach using Eq. (19). A short chain was used ($l = 15$, $G = 0.1$, $\theta \approx 29^\circ$, $b = 3.0$, and $k = 10$) and the results of Eq. (5) with pivot moves, and Eqs. (10) and (20) with bead-to-bead regrowing were compared. The configurational entropy $S(E)$ and the radius of gyration, $R_g(E)$, for all these three methods are plotted in Fig. 7. The results are in good agreement with each other.

E. Semistiff chain phase transition

Using the model described above, we could observe a phaselike transition for semistiff chains with a torsional stiffness. We applied the sampling scheme [Eq. (20)] to larger chains and investigated the conformational changes which occur with a change in temperature.

The chain lengths $l = 40$, $l = 60$, and $l = 80$ with a fixed bond length $b = 3.0$ and fixed bond angle $\theta \approx 29^\circ$, and a torsion potential [Eq. (17)] with $G = 0.10$ were used. The sampling scheme [Eq. (20)] was used during the simulation and the compactness parameter λ was chosen to sample both compact and prolonged conformations.

The graphs for

$$\langle E(T)\rangle = \frac{\sum_i E_i e^{S(E_i)-\beta E_i}}{\sum_i e^{S(E_i)-\beta E_i}} \tag{21}$$

and the heat capacity

$$C_V(T) = \frac{1}{T^2}(\langle E^2(T)\rangle - \langle E(T)\rangle^2) \tag{22}$$

for $l = 40$ are plotted in Fig. 8(a).

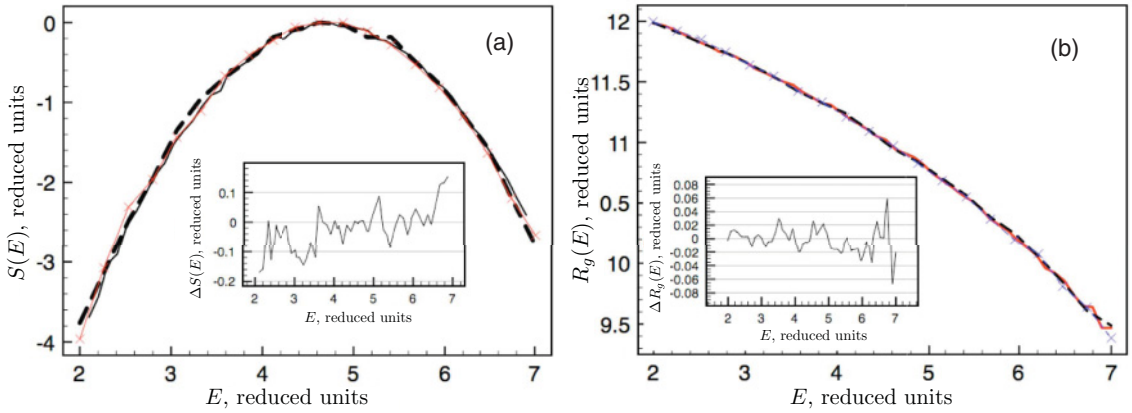

FIG. 7. (Color online) (a) Entropy dependence of the energy, $S(E)$, and (b) the energy dependence of the radius of gyration, $R_g(E)$, for the three methods: Eq. (5) (thin solid), Eq. (10) (thin crossed), and Eq. (20) (thick dashed). The system is $l = 15$, $G = 0.1$, $\theta \approx 29^\circ$, $b = 3.0$, and $k = 10$. The insets show the difference between Eqs. (5) and (20).

It should be noticed from Fig. 8, that $\langle E(T)\rangle$ experiences a rapid, but continuous change during the phaselike transition, while $C_V(T)$ has a special point as a function of temperature. So this transition can be considered as a second-order-like transition. This transition is accompanied by the collapsing of the chain: $\langle R_g(T)\rangle$ decreases by a factor of 2, while $C_V(T) \to \infty$ as seen in Fig. 8(b). The temperature point $T_c \approx 0.27$ can be considered as the phase transition temperature for the given model.

The canonical ensemble (NVT) averaged internal energy $\langle E(T)\rangle$ for $l = 40$ was compared with the values calculated from the microcanonical (NVE) ensemble by the formula

$$\frac{1}{T} = \left(\frac{\partial S}{\partial E}\right)_{l,V} \tag{23}$$

and is shown in Fig. 9(a). We can use Eq. (23) since we obtain $S(E)$ from the simulation, and we can calculate the derivative numerically. The coincidence is reasonably good but Eq. (23) gives some deviations. To estimate the errors due to system size, $\langle E(T)\rangle$ was calculated for a short chain $l = 15$, where the entropy $S(E)$ can be calculated with very good precision [see Fig. 9(b)]. One can observe some minor deviations with $l = 15$ as well, but it is mostly due to small system size, while full coincidence of the results can be expected for large l. This leads us to believe that the reasons for the deviations are the not smooth enough $S(E)$ and the not full equivalence of the (NVT) and (NVE) ensembles [28], which has been mentioned for the case of lattice polymers [7].

The heat capacity $C_V(T)$ with varying chain length $l = 40,60,80$ is shown in Fig. 10. We can also observe some additional peaks, and the nature of these should be investigated in future work.

V. DISCUSSION

The proposed method enables us to efficiently sample structures from the uncoiled to the highly compact configurations in comparison to common pivot and crankshaft moves. As a result, it is possible to investigate conformational properties of "difficult" systems, like semistiff polymers. The scheme [Eq. (20)] with a properly chosen parameter λ ensures that

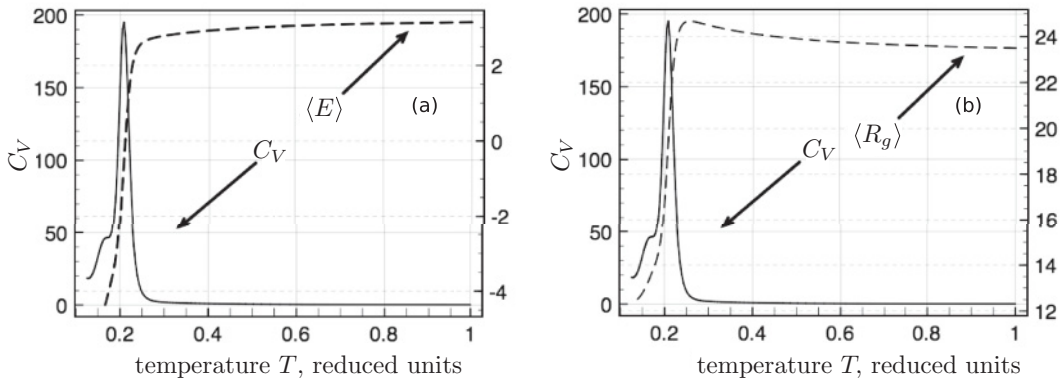

FIG. 8. (a) Specific heat capacity $C_V(T)$ as a function of temperature [Eq. (22)] (solid line) and the ensemble averaged configuration energy $\langle E(T)\rangle$ as a function of temperature (dashed line). (b) The specific heat capacity as a function of temperature, $C_V(T)$ [Eq. (22)] (solid line), and the radius of gyration as a function of temperature, $\langle R_g(T)\rangle$ (dashed line). A second-order-like transition from coil to toroid can be noticed from the behavior of $C_V(T)$ near $T_c \approx 0.2$ accompanied by the collapsing of the coil, as can be seen from the $\langle E(T)\rangle$ graph. The system is $l = 40$, $\theta \approx 29^\circ$, $b = 3.0$, $k = 20$, and $G = 0.1$.

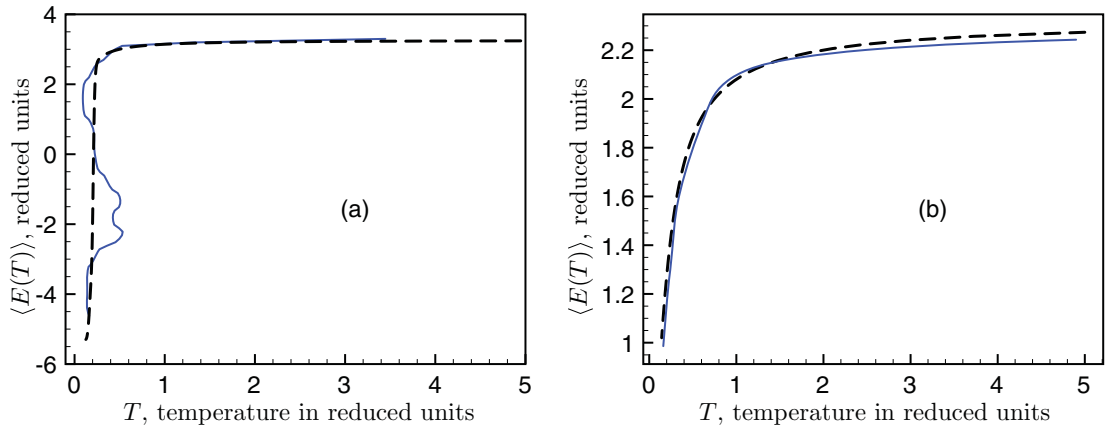

FIG. 9. (Color online) Canonical average $\langle E(T)\rangle$ with Eq. (21) (dashed line) and microcanonical with Eq. (23) (solid line) for the system: (a) $l = 40$ and (b) $l = 15$. Other parameters are $\theta \approx 29^\circ$, $b = 3.0$, $k = 40$, and $G = 0.1$.

for each energy, all (or almost all) of the configurations which correspond to that energy will be sampled. Without loss of generality, it should be possible to apply the proposed method to concentrated semistiff polymer solutions, since the principle of how the configurations are generated for a polymer in a concentrated solution remains the same, as when considering a single polymer chain.

An alternative to achieve a proper sampling in the energy space *and* in the configuration space is to build up the two-dimensional density of states $\Omega(E, R_g)$ instead of the one-dimensional $\Omega(E)$. But even in the case of $\Omega(E, R_g)$, the problem of generating configurations will remain, and some configurational biasing technique will be needed. The random pivot move will not work because it is inefficient for building up compact configurations. In any case, constructing a two-dimensional density of states will require much more computational resources.

The proposed method here has, however, to be used with some care. The most obvious case for caution is the *convergence* of the biasing function [Eq. (19)] in the energy intervals. For short chains, it works well, but the situation can become worse when increasing the chain length. The convergence might not be sufficient and some additional *smoothing* is needed. Some artifacts could be produced during the smoothing procedure. Future work includes developing even more suitable biasing functions for compact structure generation.

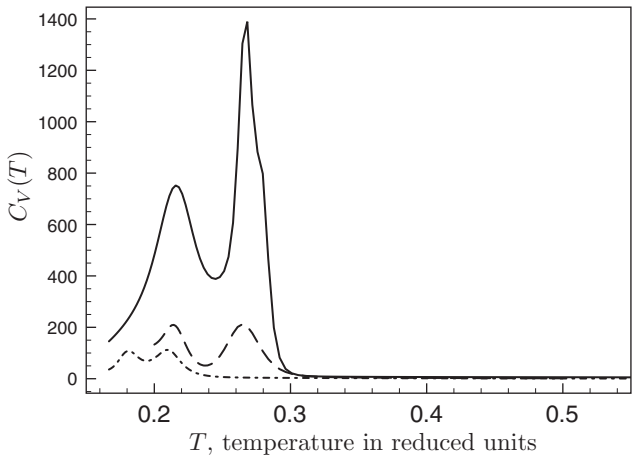

FIG. 10. Constant volume heat capacity C_V according to Eq. (22) for different chain lengths: dot-dashed line for $l = 40$, dashed line for $l = 60$, and solid line for $l = 80$. Other parameters are $\theta \approx 29^\circ$, $b = 3.0$, $k = 40$, and $G = 0.2$.

Another area for future investigation is the choice of the biasing function. In the present work, we choose the biasing function as a reduced nonbonded energy [Eq. (3)]. This is, however, not the only possible choice. Some testing was carried out for different biasing functions, e.g.,

$$w_i(\lambda) = \sum_{j=1}^{k} \exp[-\lambda r_i(j)], \tag{24}$$

where $r_i(j)$ is the distance between the ith monomer in the jth trial position and the center of mass of the *already* grown part of the chain. Depending on the compaction parameter λ, this biasing will also result in compact structures, mostly toroidal-like. For the short chains which can not form more than two loops, both biasing functions [Eqs. (2) and (24)] give the same result, but for longer chains, Eq. (24) has problems with the convergence of the biasing factors [Eq. (19)]. More fundamental work is needed in order to understand how to construct optimally behaving biasing functions.

ACKNOWLEDGMENTS

The authors thank John Grime [29] for his real-time visualization tool—Visualiser, and Eugeniy Polyakov [30] for fruitful discussions.

We acknowledge the high performance computational capacity allocated through the Swedish National Infrastructure for Computing (SNIC) on resources at the National Supercomputer Centre (NSC), alongside the UPPMAX high performance computational resources provided by Uppsala University under Project SNIC No. s00109-20. M. O. Khan acknowledges an Ingvar Carlsson Grant from the Swedish Foundation for Strategic Research.

APPENDIX

1. End-to-end distance

The correlation between bond vectors r_i and r_j for a freely-rotating chain is [31]

$$\langle r_i, r_j \rangle = l^2 (\cos\theta)^{|i-j|} = l^2 \alpha^{|i-j|} \tag{A1}$$

which means

$$\begin{aligned}\left\langle R_{ee}^2 \right\rangle &= \sum_{i=1}^{N}\sum_{j=1}^{N} l^2 \alpha^{|i-j|} = Nl^2 + 2l^2 \sum_{i=1}^{N}\sum_{k=1}^{i-1} \alpha^k \\ &= Nl^2 + 2l^2 \sum_{i=1}^{N} \alpha \left(\frac{\alpha^{i-1} - 1}{\alpha - 1} \right) \\ &= Nl^2 \left(\frac{1+\alpha}{1-\alpha} + \frac{2\alpha(\alpha^N - 1)}{N(\alpha-1)^2} \right),\end{aligned} \tag{A2}$$

where $k = i - j$ and $\alpha = \cos\theta$ substitutions were used.

2. Mean-square radius of gyration

Using

$$\left\langle R_g^2 \right\rangle = \frac{1}{(N+1)^2} \sum_{i=1}^{N} \sum_{j=i+1}^{N} \langle (R_i - R_j)^2 \rangle, \tag{A3}$$

where R_i is a radius vector of the bead i. We can use the result in Eq. (A2) to obtain [31]

$$\begin{aligned}\left\langle R_g^2 \right\rangle &= \frac{l^2}{(N+1)^2} \sum_{i=1}^{N}\sum_{j=1}^{i} |j-i| \left(\frac{1+\alpha}{1-\alpha} + \frac{2\alpha(\alpha^{|j-i|} - 1)}{|j-i|(\alpha-1)^2} \right) \\ &= \frac{l^2}{(N+1)^2} \sum_{i=1}^{N}\sum_{k=1}^{i} k \frac{1+\alpha}{1-\alpha} + \frac{2\alpha(\alpha^k - 1)}{(\alpha-1)^2} \\ &= \frac{l^2}{(N+1)^2} \sum_{i=1}^{N} \left[\frac{i(i+1)}{2} \frac{1+\alpha}{1-\alpha} + \frac{2\alpha}{(\alpha-1)^2} \alpha \frac{\alpha^{i-1}}{\alpha - 1} \right. \\ &\quad \left. - i \frac{2\alpha}{(\alpha-1)^2} \right] \\ &= l^2 N \left[\frac{(1+\alpha)}{6(1-\alpha)} \frac{N+2}{N+1} + \frac{2\alpha^3(\alpha^N - 1)}{N(N+1)^2(\alpha-1)^4} \right. \\ &\quad \left. - \frac{2\alpha^2}{(N+1)^2(\alpha-1)^3} - \frac{\alpha}{(N+1)(\alpha-1)^2} \right].\end{aligned} \tag{A4}$$

In the limit $N \to \infty$, Eq. (A4) results in the well-known relation:

$$\left\langle R_g^2 \right\rangle = \frac{l^2 N}{6} \frac{(1+\alpha)}{(1-\alpha)}. \tag{A5}$$

[1] A. Siretskiy and M. Khan, J. Phys. Condens. Matter **22**, 414103 (2010).
[2] Y. Liu and B. Chakraborty, Phys. Biol. **5**, 026004 (2008).
[3] T. Odijk, Philos. Trans. R. Soc. London A **362**, 1479 (2004).
[4] V. Bloomfield, Biopolymers **44**, 269 (1997).
[5] M. Khan and D. Chan, Macromolecules **38**, 3017 (2005).
[6] T. Jain and J. de Pablo, J. Chem. Phys. **116**, 7238 (2002).
[7] N. A. Volkov, P. N. Vorontsov-Velyaminov, and A. P. Lyubartsev, Phys. Rev. E **75**, 016705 (2007).
[8] G. Orkulas and A. Panagiotopoulos, J. Chem. Phys. **101**, 1452 (1994).
[9] M. Lal, Mol. Phys. **17**, 57 (1969).
[10] J. de Pablo, M. Laso, and W. Suter, J. Chem. Phys. **96**, 2395 (1991).
[11] M. Stevens, Biophys. J. **80**, 130 (2001).
[12] S. Burov and P. Vorontsov-Velyaminov, Mol. Phys. **104**, 3675 (2006).
[13] D. Frenkel and B. Smith, *Understanding Molecular Simulations from Algorithms to Applications*, 3rd ed. (Academic Press, San Diego, 2002).
[14] F. Wang and D. P. Landau, Phys. Rev. Lett. **86**, 2050 (2001).
[15] P. N. Vorontsov-Velyaminov *et al.*, J. Phys. A **37**, 1573 (2004).
[16] M. Taylor, W. Paul, and K. Binder, J. Chem. Phys. **131**, 114907 (2009).
[17] J. Martemyanova *et al.*, J. Chem. Phys. **122**, 174907 (2005).
[18] M. Rosenbluth and A. Rosenbluth, J. Chem. Phys. **23**, 356 (1955).
[19] J. Batoulis and K. Kremer, J. Phys. A: Math. Gen. **21**, 127 (1988).
[20] D. Frenkel, G. Mooij, and B. Smit, J. Phys. Condens. Matter **4**, 3053 (1992).
[21] Note that even in the case of steric overlapping, $u_i^r(j)$ is positive and the corresponding factor $\exp[-\lambda u_i^r(j)]$ is tiny, resulting in an extremely small probability of choosing that particular configuration.
[22] G. Ganzenmüller and P. Camp, J. Chem. Phys. **127**, 154504 (2007).
[23] The machinery of these kinds of constructions is nicely described in [13,22].
[24] Another way to understand the derivation of Eq. (10) is to notice that in Eq. (5), the probability of selecting a new configuration is unity $[\alpha(o \to n) = 1]$, since we select a new configuration randomly. But in the our case, $\alpha_R(o \to n) = \frac{e^{-\lambda(n)\Re(n)}}{W[n,\lambda(n)]}$, so we must take this into account. Writing a similar relation for $\alpha_R(n \to o)$ will result in Eq. (10).
[25] M. Rubinstein and R. Colby, *Polymer Physics* (Oxford University Press, New York, 2006).
[26] For a derivation, see the Appendix.
[27] The question of choosing of λ will be discussed in Subsec. IV B.
[28] M. Lax, Phys. Rev. **97**, 1419 (1955).
[29] [jgrime@uchicago.edu].
[30] [e.a.polyakov@gmail.com].
[31] P. J. Flory, *Statistical Mechanics of Chain Molecules* (Wiley, New York, 1969).